CRREL REPORT 91-18

Analysis of River Ice Motion Near A Breaking Front

Michael G. Ferrick, Patricia B. Weyrick, Susan T. Hunnewell

October 1991

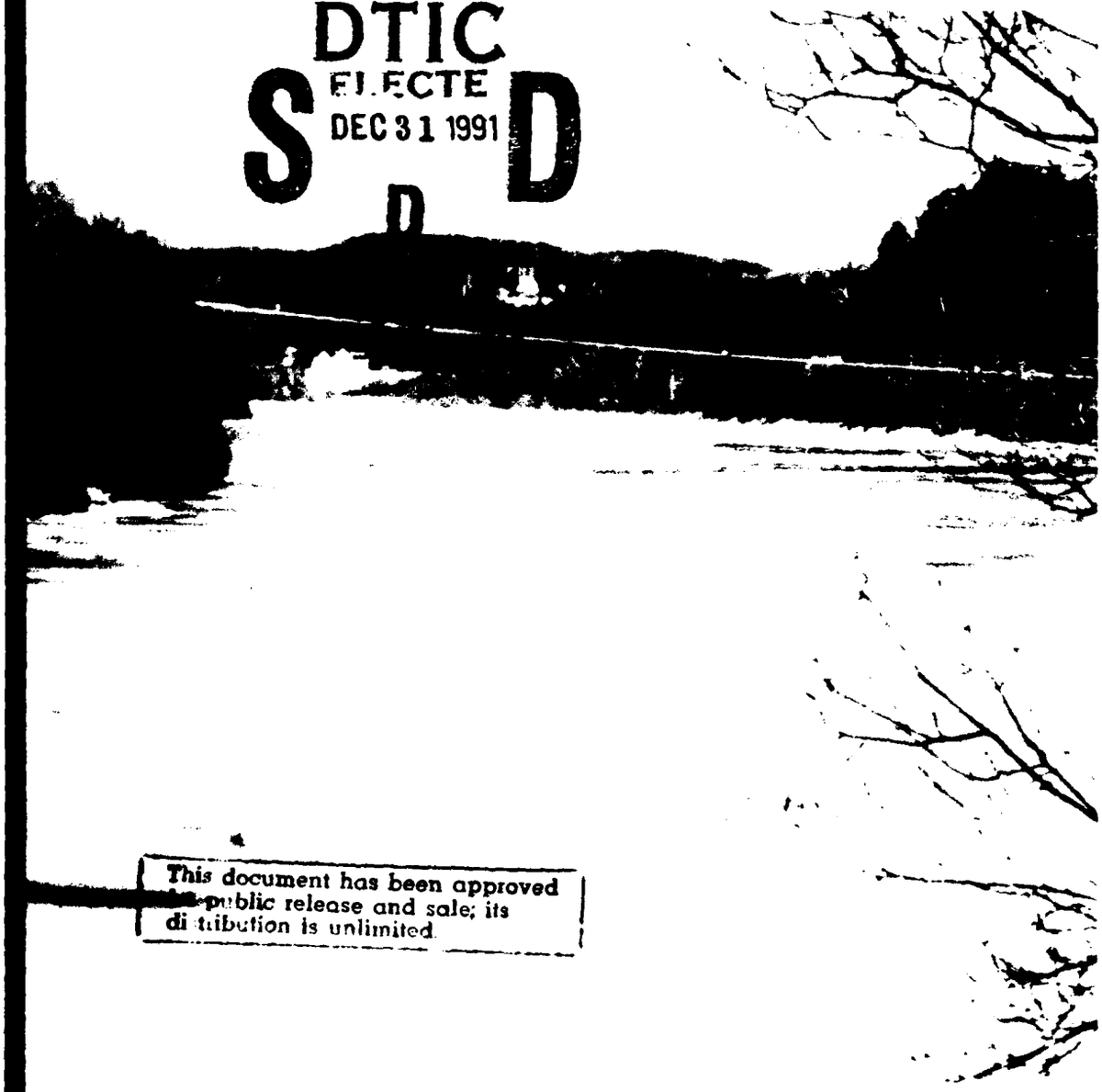

For conversion of SI metric units to U.S./British customary units of measurement consult ASTM Standard E380, Metric Practice Guide, *published by the American Society for Testing and Materials, 1916 Race St., Philadelphia, Pa. 19103.*

COVER: Looking upstream at the Connecticut River on 16 March 1989 during the controlled ice breakup experiment in Cornish, New Hampshire–Windsor, Vermont. The ice cover has an average thickness of 0.5 m and is moving from bank to bank toward the camera at a speed of about 1 m/s. Note the pressure ridge across the river and the ice rubble front (white) farther upstream. The ice temperature was 0° C and deterioration of the sheet had begun. (Photo by M. Ferrick.)

CRREL Report 91-18

U.S. Army Corps of Engineers
Cold Regions Research & Engineering Laboratory

Analysis of River Ice Motion Near A Breaking Front

Michael G. Ferrick, Patricia B. Weyrick, Susan T. Hunnewell

October 1991

PREFACE

This report was prepared by Michael G. Ferrick, Hydrologist, Patricia B. Weyrick, Physical Science Technician and Susan T. Hunnewell, Physical Science Intern, of the Snow and Ice Branch, Research Division, U.S. Army Cold Regions Research and Engineering Laboratory. Funding for this research was primarily provided by CRREL's In-House Laboratory Independent Research Program, Work Unit 90-45, *Development of a Predictive River Ice Breakup Capability,* and partially by DA Project 4A762730AT42, *Design, Construction and Operations Technology for Cold Regions,* Task CS, Work Unit 001, *River Ice Mechanics for Combat Engineering.*

The authors thank Kathleen Jones and Steven Daly of CRREL and two anonymous reviewers for their technical review of this report, Donna Harp for skill and patience in preparing many drafts, and Edmund Wright for careful editing.

CONTENTS

ILLUSTRATIONS

Figure

NOMENCLATURE

a_0, a_1, a_2, a_3	coefficients of the composite polynomial for ice velocity at a point
a, b, c, q	parameter groupings in the equation of motion for the ice
$A_I(x,t)$	acceleration of the ice
B	river width
B_i, C_i	coefficients in the recurrence relation for othogonal polynomials
C_b	speed of the breaking front
C_d	dynamic wave speed in the downstream direction
C_{*I}	dimensionless Chezy conveyance coefficient of the ice
C_m	apparent or added mass coefficient
$d_0, d_1, d_2, \ldots, d_k$	coefficients in a linear combination of orthogonal polynomials that approximate the ice velocity data
d_i^*	ith coefficient of the best least-squares fit to the data with orthogonal polynomials
E	error measure of the distance between the polynomial approximation and the data
ERROR(t_n)	the difference between the measured ice velocity and the polynomial representation at local time t_n
$f(t_n)$	the measured ice velocity at local time t_n
F_d	drag force on the ice due to fluid shear
F_g	downstream gravitational force on the ice due to its weight
F_m	acceleration reaction or force on the ice due to the apparent or added mass
F_r	force on the ice from bank resistance
g	acceleration due to gravity
$< g,h >$	scalar product between arbitrary functions g and h
I_1, I_2	integrals that are evaluated numerically
m_I	mass of ice in a control volume
$P_0, P_1, P_2, \ldots, P_k$	series of mutually orthogonal polynomials
P_i	ith polynomial in the series of orthogonal polynomials
R_I	hydraulic radius associated with the ice passing the control volume
S_i	scalar product of polynomial P_i with itself
S_f	hydraulic gradient of the river
t	global time for the ice motion in a river reach
$\tilde{t}$	local time at a point measured from the arrival of the breaking front that initiates ice motion
$\Delta\tilde{t}$	correction to $\tilde{t}$ at each step of the iterative solution
$\hat{t}$	dummy time variable of integration
t_I	ice thickness
V	flow velocity
$v_I(t)$	local ice velocity at a fixed location represented by the composite polynomial
$V_I(x,t)$	global ice velocity for the river reach
$\hat{v}_I$	dummy ice velocity variable of integration
x	position along the river reach in a fixed coordinate system
x_0, x_f	initial, final position of the ice block
x_{bf}	location of the breaking front
x_m	position of the moving coordinate system with positive distance measured upstream from the breaking front
Δx	distance between the centers of neighboring ice blocks
$w(t_n)$	weight assigned to the measured ice velocity at local time t_n
ρ	density of water
ρ_I	density of ice
τ_b	bank stress on the ice in the control volume

Analysis of River Ice Motion Near A Breaking Front

MICHAEL G. FERRICK, PATRICIA B. WEYRICK, SUSAN T. HUNNEWELL

INTRODUCTION

The characteristics of river ice breakup can vary greatly at a given site in different years, and between sites. Damages and flooding caused by breakup generally increase with river discharge and the thickness and competence of the ice cover. As the force of the river and the resistance of the ice cover increase, the processes of breakup become increasingly dynamic. In such "dynamic breakups" both the ice motion and the river flow exhibit large and rapid changes with time. The importance of unsteady flow in dynamic breakup has been noted by several authors (e.g., Beltaos and Krishnappan 1982, Billfalk 1982, Doyle and Andres 1979, Ferrick and Mulherin 1989, Henderson and Gerard 1981, Prowse et al. 1986, Williamson 1989). However, a theory of dynamic breakup that quantifies the time varying flow and ice conditions is not available. An essential part of such a theory would describe conditions near the front of the breakup.

The following description and analysis of dynamic ice breakup follows Ferrick and Mulherin (1989). The "breaking front" in a dynamic breakup is the boundary between intact stationary ice and moving ice. The breaking front travels downstream, and when it passes a given point, the local ice cover that was initially at rest also begins to move downstream. The breaking front represents a discontinuity in the ice acceleration. Ahead of the front both the ice velocity and acceleration are zero, and behind it they are both positive. The speed of the breaking front, determined by the force-resistance balance, is a function of river geometry and flow and ice characteristics. Behind this front the ice can move as a single sheet, as large plates, or as ice rubble. A second front called the "rubble front" separates the ice sheet or plates from the brash ice. The moving ice rubble behind the front extends above the downstream ice as a result of its thickness. The rubble front location represents a region of ice convergence and is readily apparent.

The characteristics of dynamic ice breakup depend on the mode of failure of the ice cover. A failure at the supports of an ice cover produces a sudden bank-to-bank release of the ice. This ice release, which we call "support-dominated dynamic breakup," travels rapidly downstream at a speed that is limited by the dynamic wave celerity, but is much greater than the flow velocity. Distinct breaking and rubble fronts accompany this type of failure, with the rubble front following the breaking front downstream. The distance between these fronts varies, depending on their relative instantaneous speeds. The breaking front in a support-dominated breakup with large plate or sheet movement is difficult to observe, a consequence of minimal ice ridging near the front. Conversely, in what we call "strength-dominated dynamic breakup," the brash ice from breakup upstream is directly involved in breaking the intact and stationary ice cover. The ice generally fails in bending caused by forces resulting from the flow and from the brash ice movement. The rubble and breaking fronts are coincident, and the speed of this combined front is usually lower than the flow velocity. However, transitions between these behaviors are common during a breakup, allowing plate collisions and size reduction ahead of the ice rubble to increase the apparent speed of the rubble front.

The motion of the ice near the breaking front during a dynamic ice breakup has not received sufficient attention. This motion and the parameters that affect it are critical for development or assessment of theories of dynamic ice breakup. In this report we develop an analysis of this motion and demonstrate the results using observed data from a controlled dynamic breakup of the Connecticut River. The known flow conditions and almost rigid body motion of the ice sheet near the front provide a relatively simple support-dominated breakup for study. We used videotape of the ice motion to identify the breaking front and to obtain a time series of ice velocity data at a cross section of the river. These data typify the time varying ice velocities that occur immediately upstream of the breaking front. An empirical expression for ice velocity was obtained that minimized the error and noise in the data and identified the primary ice motion. This methodology should be generally applicable to any dynamic breakup.

Our analysis of the ice motion relies on assumptions that extend these data at a point to a complete description of the motion in the river reach. Many of the results are sensitive to the speed of the breaking front, a parameter that was not measured locally. However, the speed of the front was varied over a wide range to explore this sensitivity. The time variations of several parameters related to the ice motion were obtained for the camera site. The variability of the ice velocity with time indicated a need to formulate and study an equation of motion for a control volume at this site. In order to more completely assess conditions near the front we also obtain the spatial variations of several parameters of the ice motion from the perspective of an observer moving with the breaking front. The analysis quantifies several concepts contained in the largely descriptive framework of ice breakup of Ferrick and Mulherin (1989).

DATA ACQUISITION

A controlled ice breakup experiment was conducted on the Connecticut River below the Wilder Dam (Ferrick and Mulherin 1989) on 15–17 March 1989. A controlled flow surge was released from the dam that caused the ice breakup to progress downstream with the front of the surge. During this experiment river stage and ice motion were recorded at several locations. Video cameras were positioned along the river bank to record the ice motion. Both stage and ice motion data were collected simultaneously at a site located 26 km downstream of the dam. The camera at the 26 km observation site remained focused on a position in the river for almost 300 s starting with the arrival of the breaking front. This segment of the tape was viewed repeatedly until the paths of ice motion were identified and drawn on a clear sheet overlying the video monitor. Points on the ice to be used for velocity measurement were chosen by their contrast from the surrounding ice. Start and stop points were selected on each ice flow line near the center of the field of view to define a measurement section. The spacing between these points was chosen to ensure a sufficient time of travel for precise and representative velocity measurements, and a length scale for each flow line was obtained from known local distances. The videotape was window dubbed with a continuous on-screen digital time marker to provide accurate and consistent travel times.

The length scale divided by the travel time through the test section provided the estimated ice velocity at the mean time of the motion (Fig. 1). The data obtained thus represent the ice velocity as a function of time at one longitudinal location in the river. Maximum measurement error bounds were 0.5 m in length and 0.5 s in elapsed time. Combining these errors unfavorably yields a maximum ice velocity error of slightly less than 7% at the peak velocity, corresponding to an absolute error of 0.08 m/s.

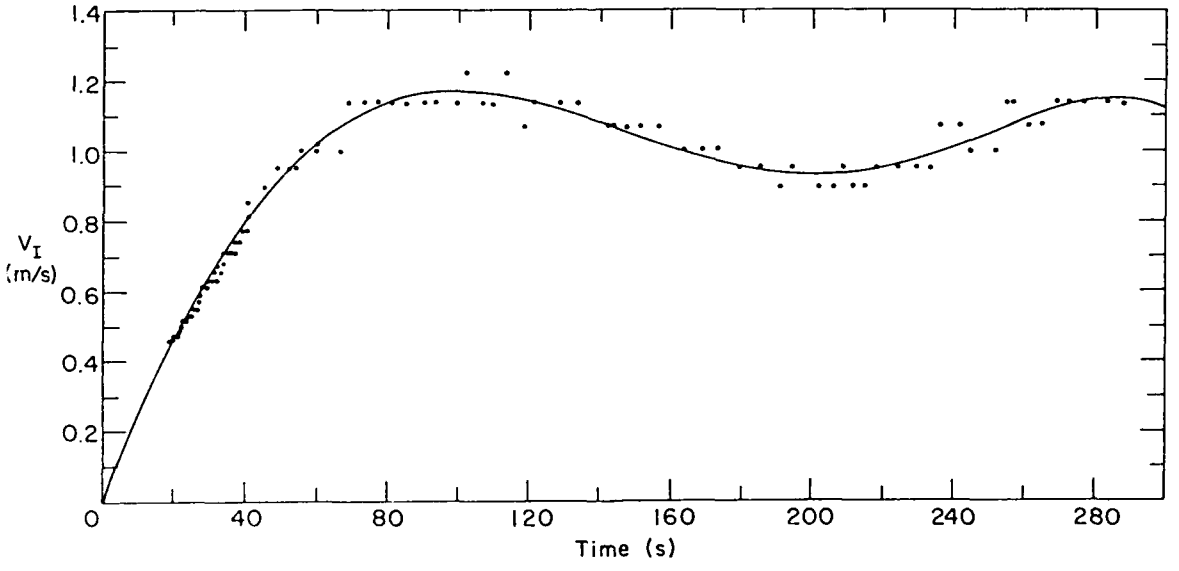

Figure 1. Ice velocity data from the controlled breakup of the Connecticut River in March 1989 and the 5th-order polynomial description of the data obtained from a least squares fit of the sequence of orthogonal polynomials.

LOCAL ICE VELOCITY POLYNOMIAL

We will now seek a continuous, differentiable function to represent the ice velocity v_I data that were obtained at the measurement section. A discrete time t_n measured from the time of breaking front arrival is associated with each ice velocity measurement. These data are represented as $f(t_n)$, indicating the measured ice velocity of the nth time in a sequence with increasing time. We assume that the measured data contain a slowly varying component that provides important information about the changes in ice velocity with time, and a comparatively rapid variation of relatively small amplitude that represents the error or noise in the data. The task is to approximate $f(t_n)$ with a function $v_I(t)$ that contains most of the information in the data and little of the error or noise. In our analysis, we used orthogonal polynomials to obtain $v_I(t)$. Details of the application of orthogonal polynomials to fitting the ice velocity data can be found in the appendix to this report, and additional background is given by Conte and deBoor (1980).

The fitted polynomial for ice velocity is obtained as a linear combination of orthogonal polynomials. We rewrite this expression as a "composite" of the orthogonal polynomials in the form

$$v_I(\tilde{t}) = a_0 + a_1 \tilde{t} + a_2 \tilde{t}^2 + a_3 \tilde{t}^3 + a_4 \tilde{t}^4 + a_5 \tilde{t}^5 + \ldots \quad (1)$$

where $\tilde{t}$ is local time measured from the arrival of the breaking front, and $a_0 = 0$ because the ice velocity is zero at $\tilde{t} = 0$. The error between the composite polynomial and the data is represented by a time series for each level of the approximation. The error between the composite polynomial and the data at any time t_n is

$$\text{ERROR } (t_n) = f(t_n) - v_I(t_n) \quad (2)$$

An appropriate degree polynomial can be found by observing both the absolute magnitude and randomness of the error. Polynomials of increasing degree incorporate additional information from the ice velocity data until the magnitude of the maximum error ceases to decrease and the structure of the error is random.

The ice velocity data were fitted with sets of orthogonal polynomials of increasing degree. Based on the error behavior, the set through degree 5 was chosen and a plot of the composite polynomial is presented with the data in Figure 1. The structure of the error is shown in Figure 2, with a root-mean-square (rms) of 0.03 m/s. Errors of this magnitude are in the expected range of measurement error. Higher degree polynomials reduced the rms error slightly, but did not reduce the maximum error nor significantly increase the random nature of the error.

ICE VELOCITY AND ACCELERATION

During dynamic river ice breakup the ice motion varies in both time and space. Data are not available to quantify the spatial changes in ice velocity near the measurement location. In this section we make assumptions concerning the ice motion that compensate for the lack of multiple ice observation points in the reach and provide a complete description of the motion. We relate the local time and ice velocity data represented by the polynomial to a "global" reach time scale, and obtain ice velocity and acceleration for the reach as functions of both time and space.

In the controlled breakup of the Connecticut River, the breaking front stalled briefly 2 km upstream of the observation site and then moved quickly through the reach. The flow disturbance caused by the ice release upstream initiated the breakup of the study reach. We

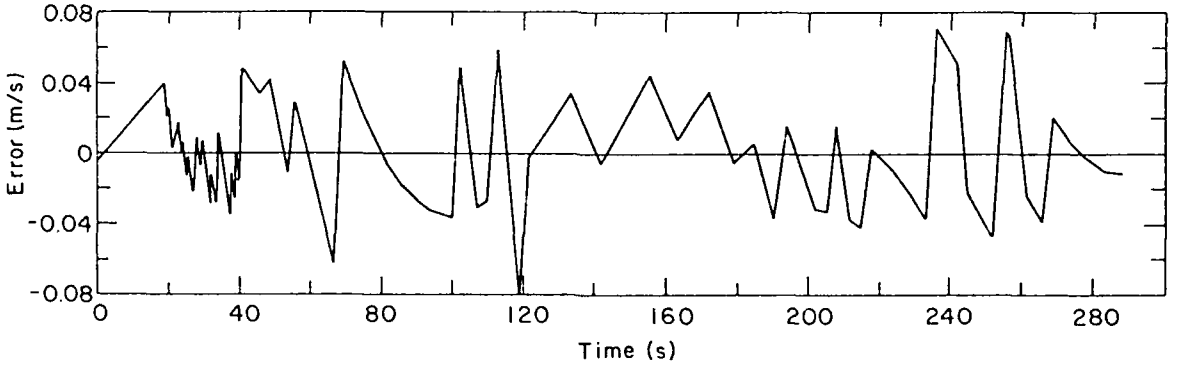

Figure 2. Structure of the velocity error associated with the 5th-order polynomial.

will make the following assumptions in order to completely specify the ice motion near the breaking front: 1) the speed of the breaking front is analogous to water wave celerity, 2) this breaking front celerity was constant as the front traveled through a reach of about 2000-m length containing the observation site, and 3) the measured ice velocity–time behavior was the same at every point in the reach when offset for different arrival times of the breaking front.

With these assumptions we know the ice velocity as a function of local time $\tilde{t}$ at every point in the reach, and local times are related by the relative spatial positions of the points and the speed of the breaking front. We arbitrarily define global time $t = 0$ to correspond to the breaking front at location $x = 0$. If C_b is the speed of the breaking front, then the front arrival at any location x occurs at $t = x/C_b$, corresponding to $\tilde{t} = 0$, and the time scales are related as

$$\tilde{t} = t - x/C_b \tag{3}$$

In differential form the time scales given in eq 3 are related as

$$\frac{d\tilde{t}}{dt} = 1 - \frac{V_I(x,t)}{C_b} \tag{4}$$

where $V_I(x,t)$ is the global velocity.

If global coordinates x and t are specified, we observe that the corresponding global ice velocity $V_I(x,t)$ can be obtained from the ice velocity polynomial as

$$V_I(x,t) = v_I(\tilde{t}) \tag{5}$$

Following from the assumptions, the ice velocity is constant along parallel, straight lines called characteristics in the x-t plane with slope

$$\frac{dx}{dt} = C_b \tag{6}$$

shown in Figure 3. Constant ice velocity along characteristics given by eq 6 can be stated as

$$\left(\frac{\partial}{\partial t} + C_b \frac{\partial}{\partial x}\right) V_I = 0 \tag{7}$$

The ice velocity polynomial defines the motion along a vertical line in Figure 3 that extends upward in time from a point corresponding to the observation site. A vertical line at any location x depicts the same time history of ice velocity following breaking front arrival. The assumptions have expanded the description of motion at a point contained in the data to include the ice motion at all points in an x-t plane drawn for the local reach.

Ahead of the breaking front the ice is stationary with zero acceleration, while behind it the ice undergoes positive acceleration and begins moving downstream.

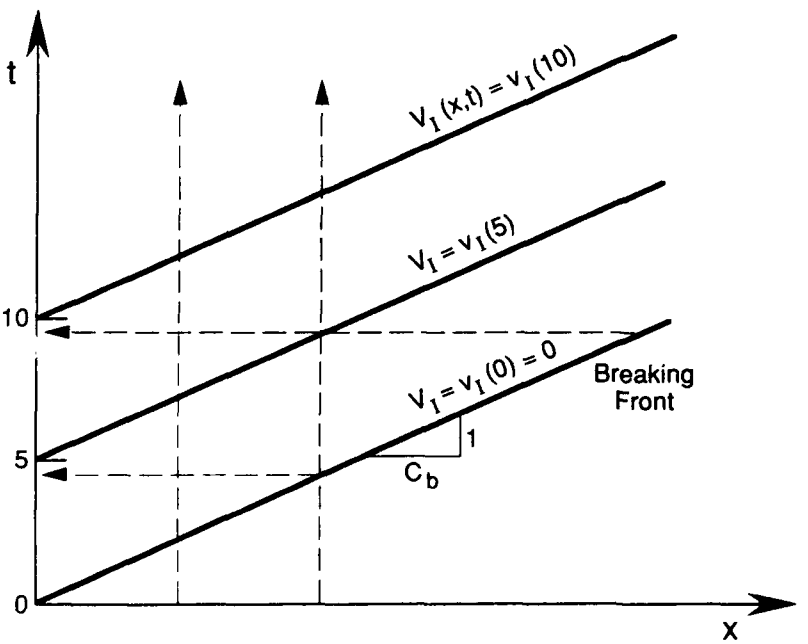

Figure 3. Sketch of the x-t plane showing selected lines of constant ice velocity including the breaking front. Ice velocities at fixed locations are the same through time, offset by the lag in breaking front arrival. Ice velocities with distance from this front are the same at any time.

The ice acceleration A_I is obtained by differentiating eq 5

$$A_I = \frac{dV_I(x,t)}{dt} = \frac{dv_I(\tilde{t})}{d\tilde{t}} \frac{d\tilde{t}}{dt} = \left(1 - \frac{v_I(\tilde{t})}{C_b}\right) \frac{dv_I(\tilde{t})}{d\tilde{t}} \qquad (8)$$

which can be evaluated using the ice velocity polynomial. The derivative of the ice velocity polynomial with respect to $\tilde{t}$ is the local ice acceleration as a function of time following the arrival of the breaking front. Alternatively, by expanding dV_I/dt and using eq 7 we obtain

$$A_I = \frac{dV_I}{dt} = \frac{\partial V_I}{\partial t} + V_I \frac{\partial V_I}{\partial x} = \frac{\partial V_I}{\partial t}\left(1 - \frac{V_I}{C_b}\right) \qquad (9)$$

With eq 5 and the observation that the local acceleration $\partial V_I/\partial t = dv_I(\tilde{t})/d\tilde{t}$, eq 8 and 9 are equivalent.

Although the speed of the breaking front near the observation site was not obtained during the field experiment, the average speed of the breaking front observed over a 12-km reach was 2.7 m/s, which included temporary stalling at a few locations. The speed of the downstream traveling dynamic wave near the observation site was 7.5 m/s. The breaking front speed can be nondimensionalized by the flow velocity at the time of breakup, and a useful range of dimensionless front speeds is from 1, corresponding to the flow velocity, to 5, corresponding to the downstream dynamic wave speed. The total ice acceleration at every point in the reach is presented as a function of time in Figure 4 for dimensionless breaking front speeds of 2 and 5. The zero time in this figure corresponds to the local arrival of the breaking front. The behavior of these curves is the same except that the absolute value of the total acceleration increases slightly as C_b increases. The maximum acceleration occurred with the initial motion, decreasing rapidly in the first minute. For the remainder of the record, acceleration oscillated about zero.

EQUATION OF MOTION FOR ICE

We will now write a simplified equation of motion for the ice cover that can be solved analytically, and begin to quantify the effects of various parameters on the ice motion. In this initial study we consider the forces on the ice due to the flow but, for simplicity, we neglect the response of the flow to the ice motion. The variations in flow parameters caused by ice breakup will be quantified in future work.

The flow discharge, depth and velocity were all increasing through the period of ice velocity measurement. The rate of increase of river stage was constant through the period, but the increase in the flow depth was only a few percent of the initial value. We assume that during the measurement period the water surface profile of the surge that caused the breakup moved downstream as a monoclinal wave with constant speed and unchanging shape. This constant rate of stage increase thus produces a constant energy gradient. With constant depth and energy gradient our calculations indicate an increase in the flow velocity of about 25% of the initial value during the measurement period. The

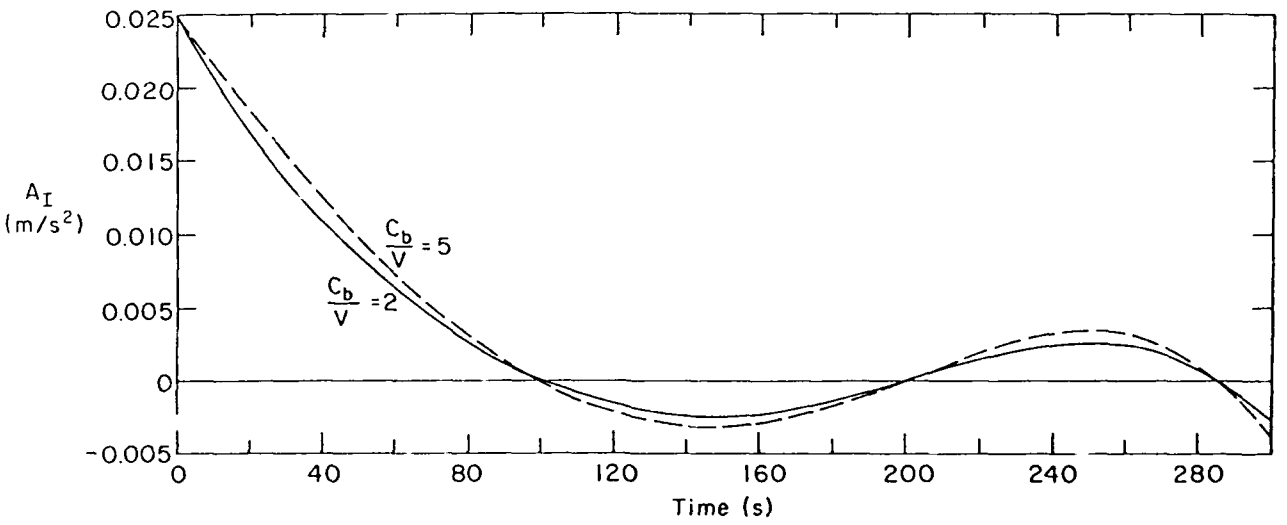

Figure 4. Total ice acceleration at the observation site for assumed dimensionless breaking front speeds of 2 and 5.

increase in flow velocity is in response to diminished resistance to flow as the ice accelerates. However, the assumption of constant velocity at the mean value will be made to simplify the analysis without introducing a large error.

During the breakup experiment on the Connecticut River the sheet broke apart downstream of the measurement location and provided negligible resistance to the moving ice upstream. When the ice run finally stalled, the river was open downstream of the observation site. Also, force dissipation internal to the ice sheet caused by ridging away from the banks was not common near the breaking front. Therefore, we can neglect downstream support and internal force dissipation and attribute all ice motion resistance to the river banks. Because of daily and seasonal changes in river stage, the ice sheet exhibited well-developed shore cracks near each bank prior to the controlled breakup. These cracks were roughly parallel to the banks, but highly irregular. There was no connection between the cover and the banks at some locations, and rigid interlocking with shorefast ice at others. To obtain a tractable equation of motion we neglect the forces transmitted through the cover in the longitudinal direction, and consider the bank resistance term as typical or locally averaged. Following the arrival of the breaking front, the ice fractured into small pieces near the banks to allow the primary sheet or floes to pass. The amount of fracturing depended on the size of these large ice forms relative to the local river width, and appeared to vary with time. These processes represented an energy loss to the moving ice that we will lump into the bank resistance.

Consider a stationary control volume that spans the river cross section at the measurement location and has a unit length in the longitudinal direction. The reason for this choice of width is that the sizes of the ice sheet or plates were on the order of the river width. The unit length is arbitrary, but consistent with the typical or averaged force balance. The equation of motion for the ice in this control volume can be written as

$$F_m + F_d + F_g - F_r = m_I \frac{dV_I}{dt} \qquad (10)$$

where

F_m = acceleration reaction or force due to the apparent or added mass
F_d = drag force on the ice due to fluid shear
F_g = downstream gravitational force due to the weight of the ice
F_r = bank resistance force
m_I = mass of ice in the control volume.

The force due to apparent mass can be parameterized as

$$F_m = -C_m \left(m_I \frac{dV_I}{dt} \right) \qquad (11)$$

where C_m is an apparent mass coefficient to be determined experimentally or approximated analytically. Wake et al. (1987) performed a set of experiments on ice floes with various aspect ratios and found $C_m = 0.1$ for floes that are large relative to their thickness.

The drag force on the ice due to fluid shear will be parameterized using a hydraulic radius. An idealized vertical profile of water velocity in an ice covered channel exhibits a zero velocity at each boundary and a maximum velocity near mid-depth. The precise location of the maximum depends on the relative roughnesses of the cover and the bed. Physically, the hydraulic radius associated with the ice cover is the distance from the ice to the velocity maximum, and the remainder of the depth is the hydraulic radius associated with the bed. The hydraulic radius associated with the ice $R_I(x,t)$ is obtained from the Chezy equation as

$$R_I(x,t) = \frac{(V - V_I(x,t)) \mid V - V_I(x,t) \mid}{g C_{*I}^2 S_f} \qquad (12)$$

where

C_{*I} = dimensionless Chezy conveyance coefficient associated with the ice
g = acceleration due to gravity
V = flow velocity
S_f = hydraulic gradient.

The drag exerted by the cover on the flow is diminished during breakup when $V_I > 0$.

With the parameterization of Ferrick and Mulherin (1989) for bank resistance, we can now rewrite eq 10 as

$$\rho g B S_f \left[R_I + \frac{\rho_I}{\rho} t_I \right] - 2 t_I \tau_b = \left(1 + C_m \right) m_I \frac{dV_I}{dt} \qquad (13)$$

where

ρ, ρ_I = density of water and ice, respectively
B = river width
t_I = ice thickness
m_I = $t_I B \rho_I$
τ_b = bank stress on the ice.

When the resistance term in eq 13 is small, the downstream component of the weight of the ice can cause V_I to exceed V, indicating a negative R_I and downstream drag of the ice on the water instead of resistance to the flow.

The physical parameters ρ, ρ_I, B, C_{*I}, t_I and the hydraulic parameters S_f and V are assumed constant at their mean values for the initial 300 s of ice motion. The density of water at 0°C was known, and river width, ice

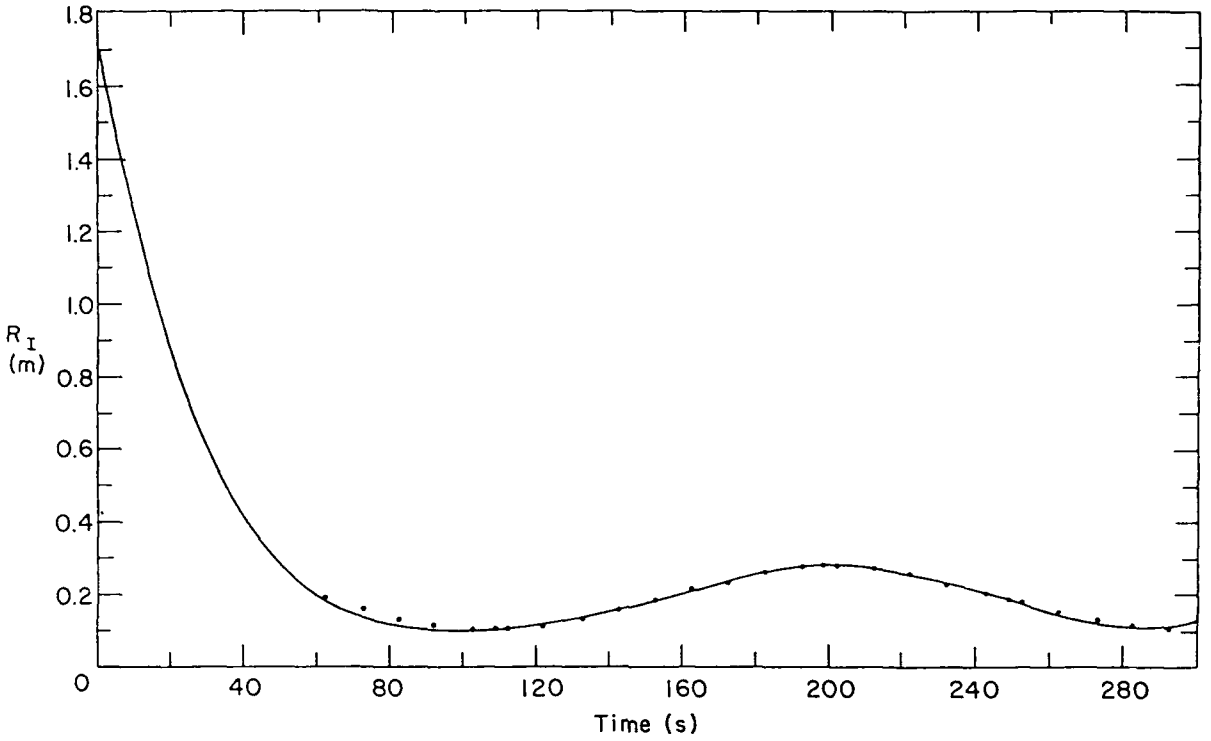

Figure 5. Hydraulic radius associated with the ice following the passage of the breaking front. The points are given by $R_I = 0.19 + 0.085\ sin[\pi + (2\pi/185)(t - 62)]$.

thickness and ice density were measured immediately prior to the experiment. These measured parameters displayed minor variability relative to their mean values through the reach. The ice, bed and combined channel conveyances for the reach were obtained by calibrating the model of Ferrick and Mulherin (1989) against data for both open water and ice covered flow conditions. The mean energy gradient and flow velocity values were estimated using both model calculations and field measurements.

The hydraulic radius associated with the ice passing the control volume was found from eq 12 and is presented in Figure 5. R_I diminished dramatically during the first minute of ice motion, and then slowly oscillated in the 0.1- to 0.3-m range for the remainder of the record. The rapid decrease in R_I for the control volume demonstrates that the flow is affected by the ice motion, and as mentioned, further work that quantifies this coupling at breakup is needed. The resistance to ice motion prevented the ice velocity from reaching the flow velocity, and R_I did not go to zero. The oscillating segment of the data is closely approximated by a sine function about a mean of 0.19 m, with an amplitude of 0.085 m and a period of 185 s. The lack of any attenuation over more than a complete period indicates either an underdamped response of the ice to a disturbance or continuous forcing of the ice velocity oscillation. A free vibration of a system is the result of a temporary initial excitation that is then attenuated by damping in the system. Alternatively, the harmonic oscillations in a forced vibration are maintained by the forcing function. We do not expect that any of the variables taken as constants caused the periodic behavior.

TEMPORAL SOLUTIONS FOR ICE VELOCITY AND BANK STRESS

In this section we will address the question of whether the oscillations in the ice velocity indicate a free or a forced vibration by developing solutions of the equation of motion subject to the constant parameter approximations at mean values. Initially, we will remove the time dependence from the equation by taking $dV_I/dt = 0$, and obtain equilibrium ice velocity as a function of bank resistance. Analytical solutions of the complete equation are then developed for initial conditions of ice at rest and arbitrary positive and negative disturbances from an equilibrium condition. None of these solutions exhibit ice velocity oscillations with time. Finally, we

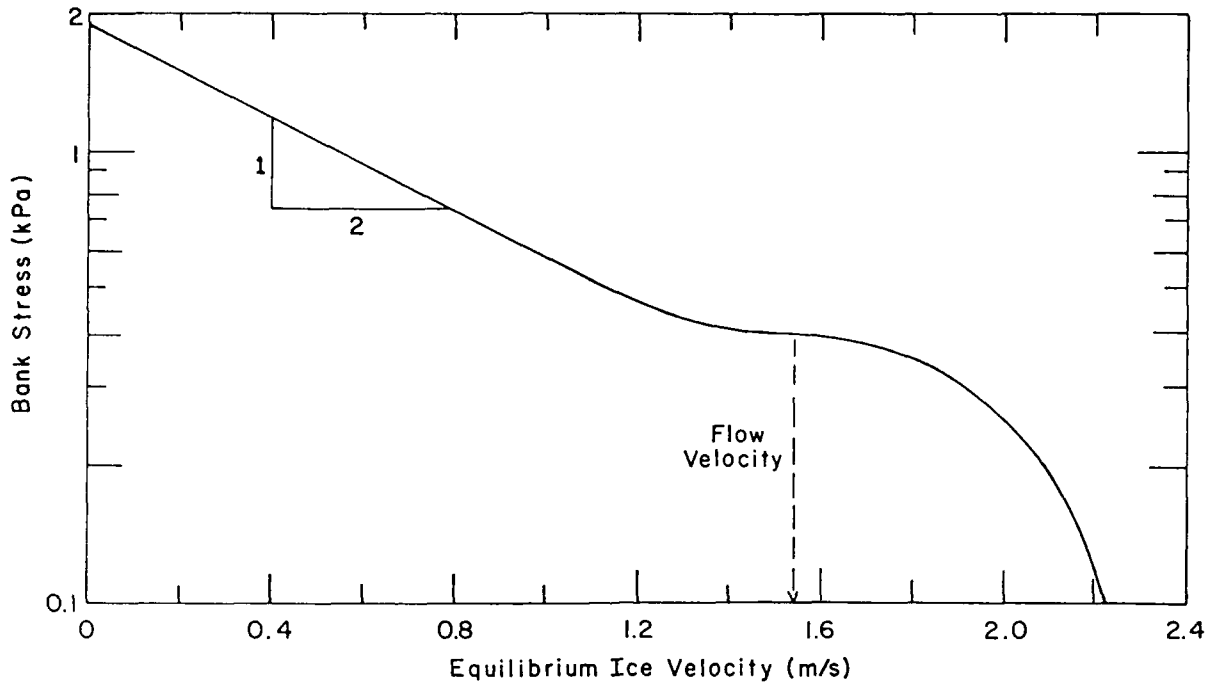

Figure 6. Equilibrium ice velocity at the observation site as a function of bank stress.

solve the equation of motion algebraically for bank resistance as a function of time, given ice velocity and acceleration from the measured data and eq 5 and eq 8. Continuously changing bank resistance was the most likely cause of the ice velocity oscillations contained in the data.

Equilibrium ice velocity as a function of bank stress is presented in Figure 6 for the hydraulic conditions present at the time of ice breakup at the observation site. At a bank stress of 0.391 kPa the equilibrium ice velocity is equal to the flow velocity. The maximum bank stress of 1.87 kPa corresponds to an ice velocity of zero, and zero resistance corresponds to a maximum ice velocity of 2.33 m/s. The constant slope of much of this curve follows because the bank stress is a negative quadratic function of the ice velocity until V_I approaches V.

In most cases of sheet and plate motion during breakup, the ice velocity is lower than the flow velocity, and eq 13 can be rewritten as

$$cV_I^2 + bV_I + a = (1 + C_m)\, m_I \frac{dV_I}{dt} \qquad (14)$$

where

$$a = \frac{\rho BV^2}{C_{*I}^2} + \rho_I g B\, S_f t_I - 2\, t_f \tau_b$$

$$b = -2\,\rho BV/C_{*I}^2$$

$$c = \rho B/C_{*I}^2 = -\frac{b}{2V}$$

$$q = 4ac - b^2 < 0$$

We are primarily interested in the solution for ice velocity at a point because these results can be directly compared to the ice velocity polynomial. Therefore, $V_I(x,t)$ and dV_I/dt in eq 14 are replaced with $v_I(\tilde{t})$ and $dv_I/d\tilde{t}$ using eq 5 and 8, and eq 14 simplifies to an ordinary differential equation in local time $\tilde{t}$ as

$$cv_I^2 + bv_I + a = (1 + C_m)m_I\left(1 - \frac{v_I}{C_b}\right)\frac{dv_I}{d\tilde{t}} \qquad (15)$$

Note that local time $\tilde{t} = 0$ can be chosen to coincide with the arrival of the breaking front, or it can be given an arbitrary definition, and $v_I(\tilde{t})$ is a general local ice velocity. With constant physical and hydraulic parameters at their mean values we can separate variables in eq 15 and write

$$\int_0^{\tilde{t}} d\hat{t} = \frac{(1 + C_m)\, m_I}{C_b} \int_{v_{I_0}}^{v_I} \frac{\left(C_b - \hat{v}_I\right) d\hat{v}_I}{c\hat{v}_I^2 + b\hat{v}_I + a} \qquad (16)$$

where $\hat{t}$ and $\hat{v}_I$ are variables of integration, and the limits

of the integrals indicate corresponding local times and ice velocities at the control volume.

We initially integrate eq 16 for the case of $v_I << C_b$ and obtain

$$\tilde{t} = (1 + C_m)\, m_I \left(\frac{-2}{\sqrt{-q}}\right) \left[\tanh^{-1} \frac{2c\hat{v}_I + b}{\sqrt{-q}}\right]_{v_{I_0}}^{v_I} \quad (17)$$

where v_{I_0} is the ice velocity at $t = 0$. After some manipulation, eq 17 can be inverted to obtain v_I as a function of time:

$$v_I = \frac{v_{I_0} + \frac{A_1\sqrt{-q}}{2c}\left(1 - \frac{bA_2}{\sqrt{-q}}\right)}{1 + A_1 A_2} \quad (18)$$

where

$$A_1 = \tanh\left(\frac{\sqrt{-q}\,\tilde{t}}{(1 + C_m)\, m_I (-2)}\right)$$

$$A_2 = \frac{2cv_{I_0} + b}{\sqrt{-q}}$$

Integration of eq 16 without simplification yields

$$\tilde{t} = (1 + C_m)\, m_I \left(\frac{-2}{\sqrt{-q}}\right)\left(1 + \frac{b}{2cC_b}\right)\left(\tanh^{-1} \frac{2c\hat{v}_I + b}{\sqrt{-q}}\right)_{v_{I_0}}^{v_I} \quad (19)$$

$$- (1 + C_m)\, m_I \left(\frac{1}{2cC_b}\right) \ln \left(c\hat{v}_I^2 + b\hat{v}_I + a\right)_{v_{I_0}}^{v_I}$$

This equation for $\tilde{t}$ as a function of v_I is not readily inverted. However, the solution expressed by eq 19 can be obtained for all ice velocities except the equilibrium value. At equilibrium the ice velocity does not vary with time, and the one-to-one correspondence between v_I and $\tilde{t}$ no longer applies. The solution of the equation of motion can be obtained similarly for the case of $V_I > V$.

The solutions expressed in eq 18 and eq 19 are presented in Figure 7 for an initial ice velocity of zero, several values of bank stress, and dimensionless breaking front speeds of 2, 5 and ∞. As the dimensionless breaking front speed decreases the approach to equilibrium occurs more rapidly if all other parameters are the same. The analytical solution closely approximates the ice velocity data with $\tau_b = 0.55$ kPa, except for the

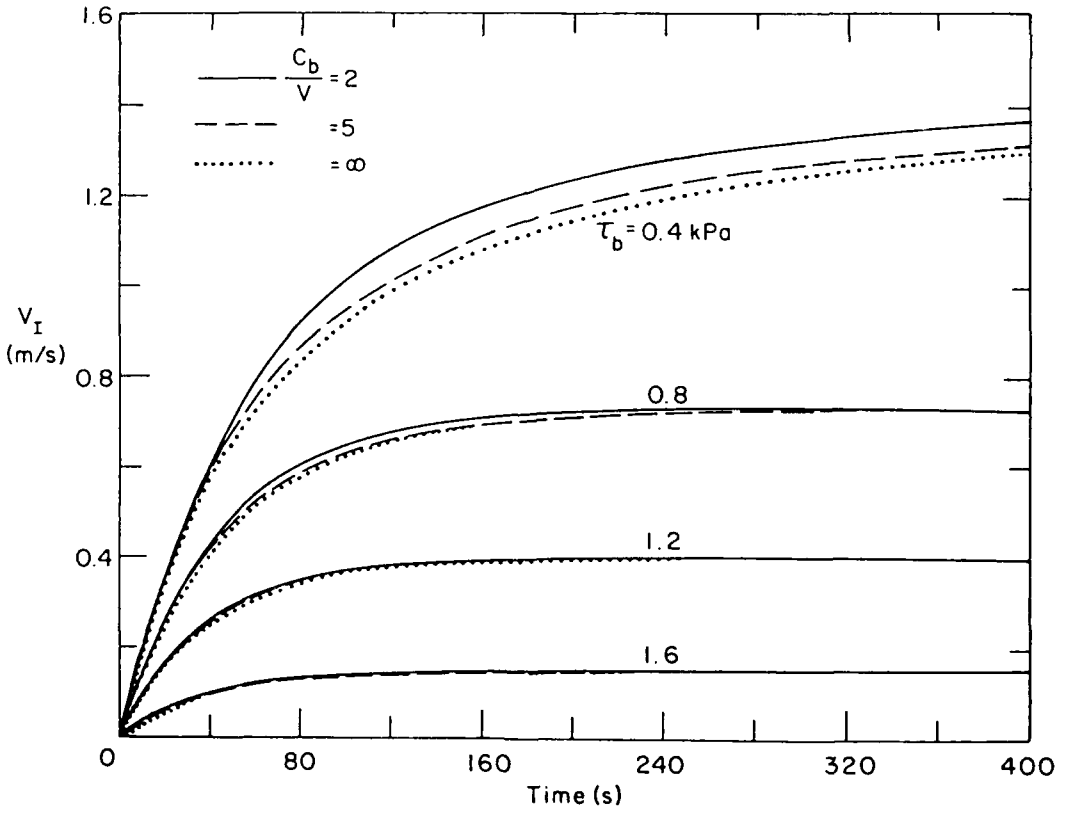

Figure 7. Analytical solution for the increase in ice velocity from rest as a function of time for several values of bank resistance and several dimensionless breaking front speeds.

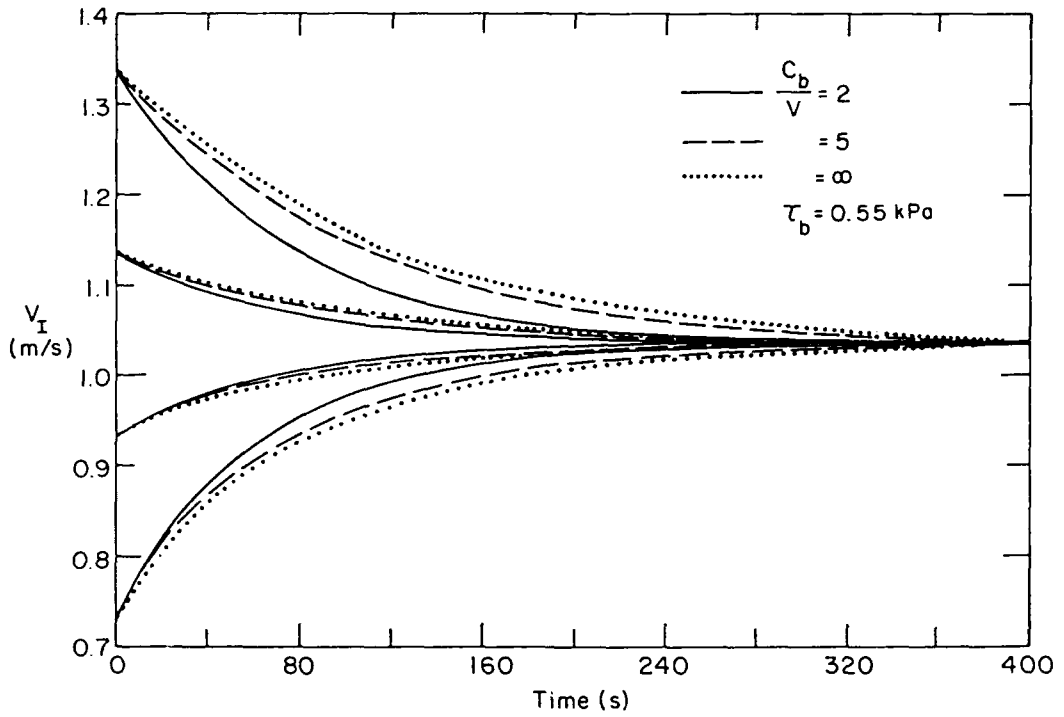

Figure 8. Analytical solution for the return to equilibrium after positive and negative initial disturbances for a single bank resistance and several dimensionless breaking front speeds.

velocity oscillations. These same solutions are given in Figure 8 for this value of bank stress and four arbitrary initial ice velocities that represent positive and negative disturbances from equilibrium. The relative behavior of these solutions follows that of the curves in Figure 7.

In order to understand these results we consider two breakup conditions with the same local velocity and local acceleration behavior, and with all parameters equal except for the breaking front speed. As the speed of the breaking front decreases, approaching the ice velocity, spatial changes in the ice velocity increase, and the total acceleration and the effective inertia of the ice are reduced (eq 15). Under these conditions equilibrium is quickly reestablished following a disturbance, and therefore, this equilibrium is very stable. Conversely, increasing C_b corresponds to increasing the inertia of the ice, and increased time to restore equilibrium. There are no oscillations of the ice velocity with time in any of these solutions.

Numerical model results of Ferrick and Mulherin (1989) indicate that the bank stress τ_b increases with time in response to the arrival of a flow surge, reaching a maximum at the arrival of the breaking front. We can develop curves of bank stress with time beginning at $\tilde{t} = 0$ for the observation site from eq 15 , given the ice velocity and acceleration relations as input. The results are presented in Figure 9 for apparent mass coefficient values of 0.0 and 0.1 and dimensionless breaking front speeds of 2 and 5, covering the range of probable parameter values. These curves are very similar, with the greatest differences early in the motion when the ice acceleration was near its maximum value. The minimum bank resistance occurred at about 30 s into the motion. After this initial period the bank shear is out of phase with the ice acceleration and precedes changes in ice velocity. The maximum bank stress in this record was about 38% of that preceding the failure, causing ice deceleration and increasing R_I. Continuously changing bank shear due to variable ice plate size was a likely cause of variable ice velocity, and it is the only process in this model that can account for this variability.

Due to the river control operations, the discharge and the downstream force on the ice gradually diminished following the period of ice velocity measurement. At 17 minutes after the arrival of the breaking front, the ice plate motion arrested at the measurement location. The stall occurred at the peak river stage, with known R_I and S_f closely approximated by the bed slope. The bank stress at the stall can be estimated using eq 13 as 1.53 kPa, about 82% of that prior to the initial motion. A large flow release on the following day yielded a slightly higher stage at the downstream force peak with $\tau_b = 1.59$ kPa, and the large plates did not fail. We conclude that large hydraulic forces were the cause of the ice motion

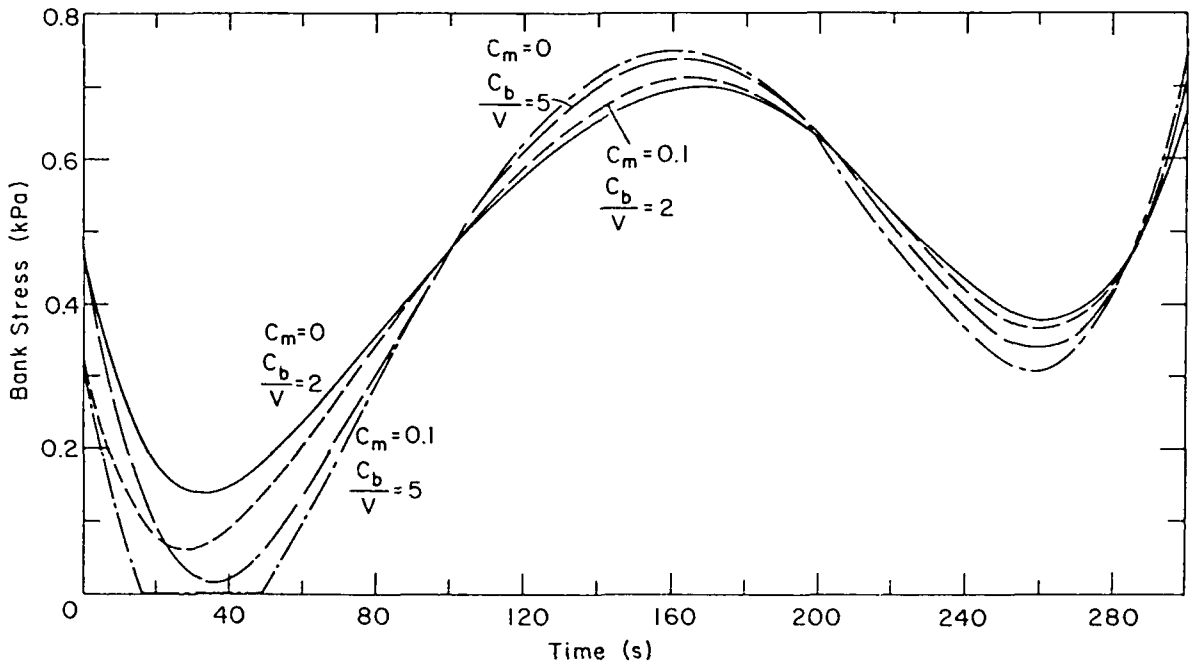

Figure 9. Bank stress following the passage of the breaking front at dimensionless speeds of 2 and 5, both considering and neglecting the force due to apparent mass.

and not simply high river stage. The eventual stall of the run was due to both diminishing forces and high bank resistance.

SPATIAL VARIATIONS NEAR THE BREAKING FRONT

We will now examine the spatial variation of several parameters that describe the ice motion near the breaking front. An analysis of the spatial variability complements the earlier one that provided temporal changes, and completes the description of the ice motion. Spatial variations of motion parameters behind the breaking front are related to those in time at a point. In Figure 3 we observe that the ice position, velocity, and acceleration upstream of the breaking front become constant in time when spatial position is relative to the front. The lack of ice ridging and rubbling near the front in the field indicates that the ice sheet was not undergoing significant ice convergence. We find that ice convergence local to the breaking front depends on the speed of the front, and note the implications of this result on breakup behavior.

In order to obtain the state of motion of an ice block, the total time of motion t must be related to $\tilde{t}$, the time since the passage of the breaking front at the present location of the block. These time scales are related in integral form from eq 4 as

$$t = C_b \int_0^{\tilde{t}} \frac{d\hat{t}}{C_b - v_I(\hat{t})} = I_1 \tag{20}$$

where $t = 0$ is defined as the time of initial motion of the block and $\hat{t}$ is a dummy variable of integration. We observe that t in eq 20 is known, the unknown $\tilde{t}$ appears as the upper limit of the integral and $\tilde{t} < t$. The solution for $\tilde{t}$ can be obtained by trial, starting from an initial estimate $\tilde{t} = (1 - v_I(t)/C_b)t$, and repeatedly applying corrections until $I_1 = t$. The correction to $\tilde{t}$ at each iteration is

$$\Delta\tilde{t} = \left(1 - \frac{v_I(\tilde{t})}{C_b}\right)(I_1 - t) \tag{21}$$

and the updated value is obtained as $\tilde{t} = \tilde{t} - \Delta\tilde{t}$. The degree of the polynomial represented by $v_I(\hat{t})$ in eq 20 will depend on the data. Therefore, we evaluate I_1 using Gaussian quadrature with limits changed to the standard interval (−1,1):

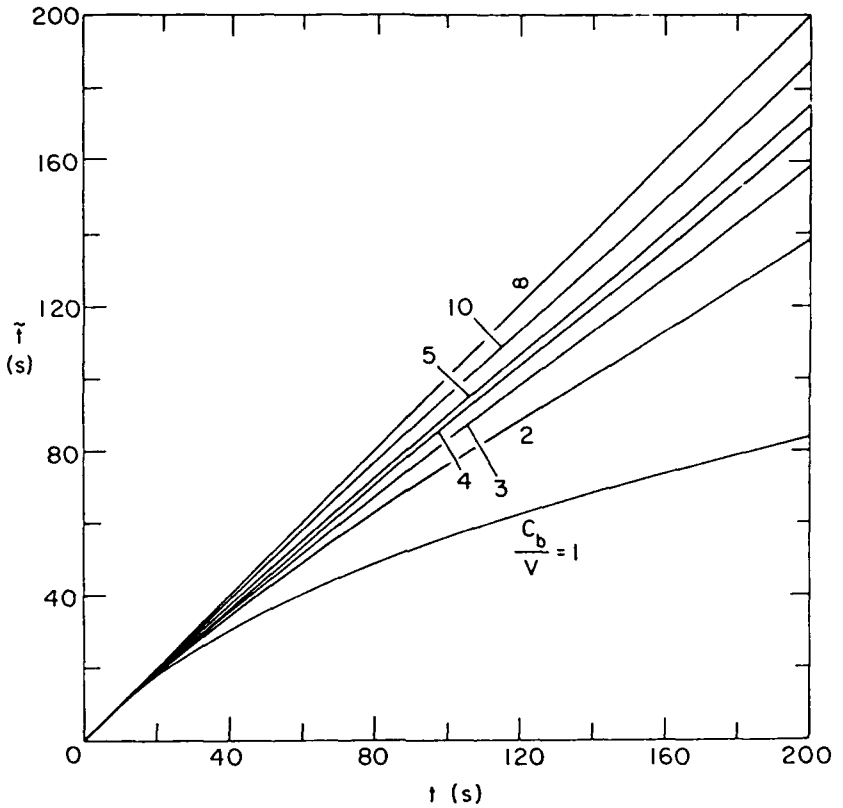

Figure 10. Time $\tilde{t}$ since the breaking front passed the final block position as a function of the time of block motion t for a range of dimensionless breaking front speeds.

$$I_1 = \frac{C_b \tilde{t}}{2} \int_{-1}^{1} \frac{d\hat{t}}{\left(C_b - v_I\left[\frac{\tilde{t}}{2}\left(\hat{t}+1\right)\right]\right)} \qquad (22)$$

The time $\tilde{t}$ as a function of the time of block motion t is given in Figure 10 for the Connecticut River ice velocity polynomial and a range of dimensionless breaking front speeds. At small values of time and for large values of C_b/V, the two time scales are nearly the same. However, for small dimensionless front speeds, these time scales diverge with increasing time.

The position of an ice block that has been in motion for time t can be obtained by relating position and velocity and then changing the variable of integration with eq 4 and 5

$$\int_{x_o}^{x_f} dx_I = \int_0^t V_I(x,t)\,dt = C_b \int_0^{\tilde{t}} \frac{v_I(\hat{t})}{C_b - v_I(\hat{t})}\,d\hat{t} = I_2 \qquad (23)$$

Given t the corresponding value of $\tilde{t}$ is known from eq 20–22, and the limits of integration in I_2 are specified. The final block position x_f can then be obtained explicitly given the initial position x_o. As before, I_2 is evaluated using Gaussian quadrature on the standard interval (–1,1). The final position of a block relative to the breaking front can be determined from the time of motion and speed of the front together with the final position of the block, or from the speed of the front and t at the final position of the block. The velocity of this ice block follows from eq 1, and block acceleration is obtained from eq 8 .

The river ice sheet is idealized as a collection of independent blocks initially at rest with known fixed coordinate positions x, and having a uniform initial spacing Δx_o. A moving coordinate system x_m traveling with the breaking front passes $x = 0$ at global time $t = 0$. The moving distance coordinate is positive upstream from the breaking front, and the fixed and moving systems are related as

$$x = x_{bf} - x_m \tag{24}$$

where the breaking front location in the fixed system $x_{bf} = C_b t$. Comparing eq 24 with eq 3 we observe that $x_m = C_b \tilde{t}$, where $\tilde{t}$ is the local time at position x. Given a dimensionless breaking front speed and the local time $\tilde{t}$ at the final position of a block, the corresponding distance from the front is known and a spatial view of any parameter can be obtained. We will track many blocks from stationary initial positions to a location and a state of motion at a later time. The results obtained below are all presented with distance x_m from the breaking front.

The time of block motion as a function of distance from the breaking front is presented in Figure 11 for a range of dimensionless speeds of the front. As the front speed approaches the flow velocity, the time of motion rapidly increases immediately behind the breaking front. Blocks that are in motion for a long time experience many collisions and typical sizes are greatly reduced. As the speed of the front increases, the time of block motion at a comparable distance from the front diminishes, allowing fewer opportunities for collisions and resulting in larger typical sizes. A block that has been in motion for 100 s behind a front with a dimensionless speed of 5 is about 8 times farther from the front than the same block in a breakup with a front speed of 1.

Ice velocity and acceleration as a function of distance behind the breaking front are given in Figures 12 and 13, respectively, for a range of dimensionless front speeds. As can be seen in Figure 12, the spatial ice velocity gradient decreases as the speed of the breaking

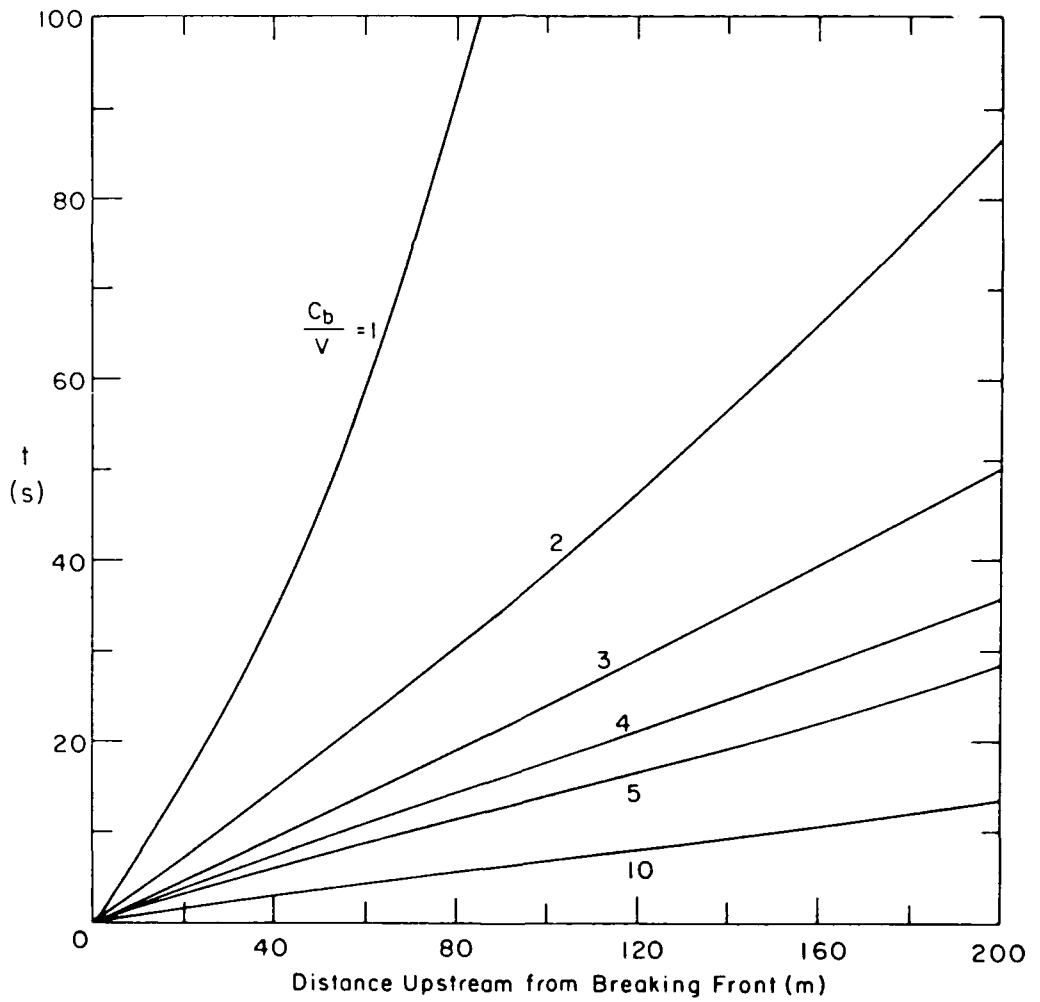

Figure 11. Time of block motion as a function of distance behind the breaking front for a range of dimensionless speeds of the front.

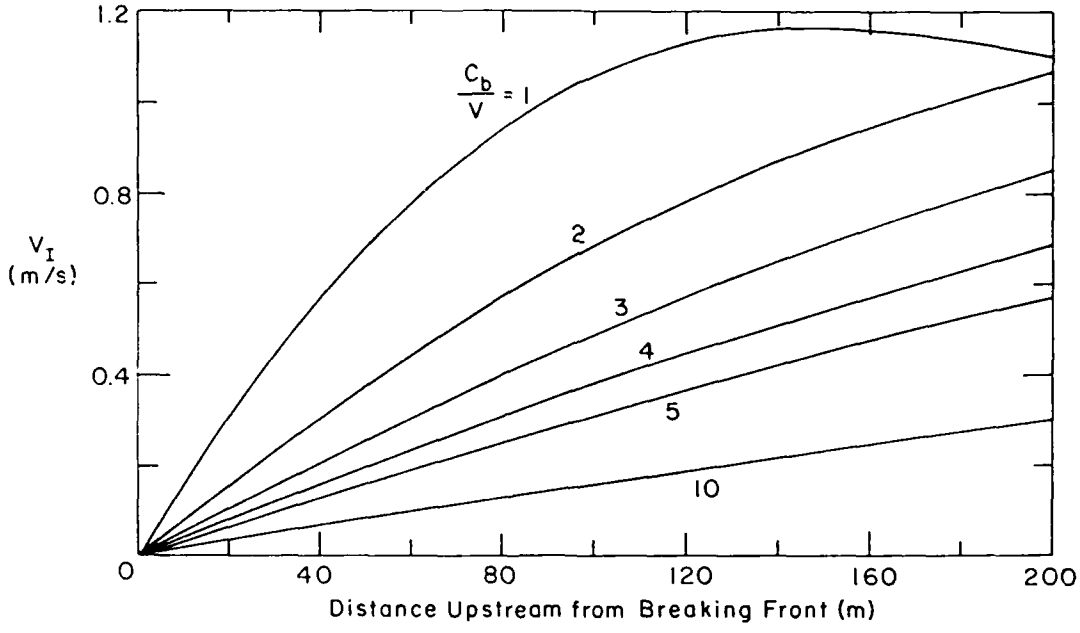

Figure 12. Ice velocity as a function of distance behind the breaking front for a range of dimensionless speeds of the front.

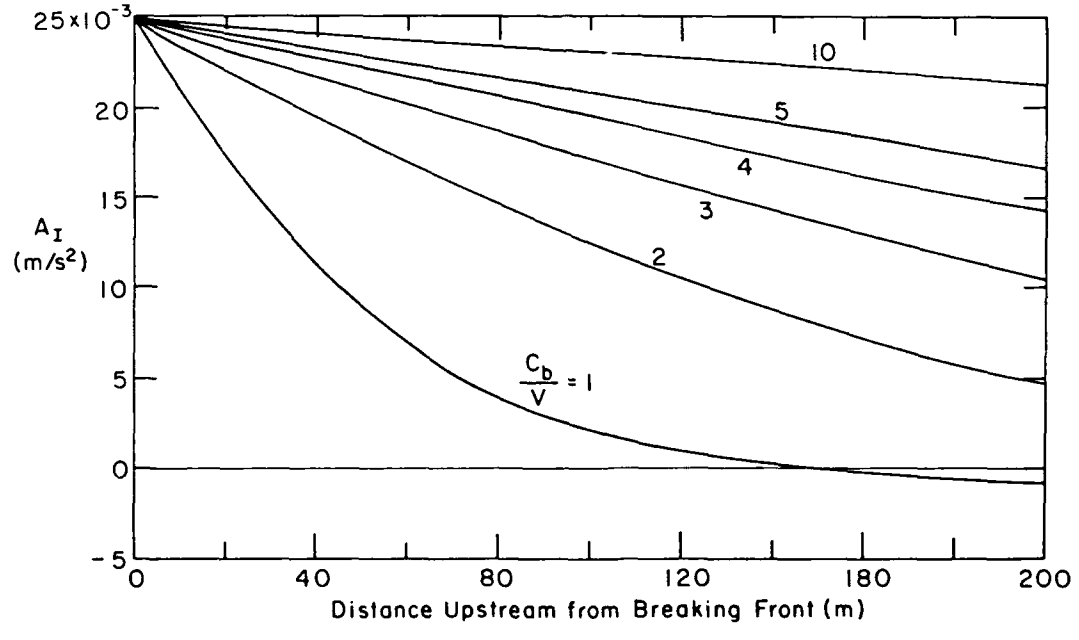

Figure 13. Total acceleration as a function of distance behind the breaking front for a range of dimensionless speeds of the front.

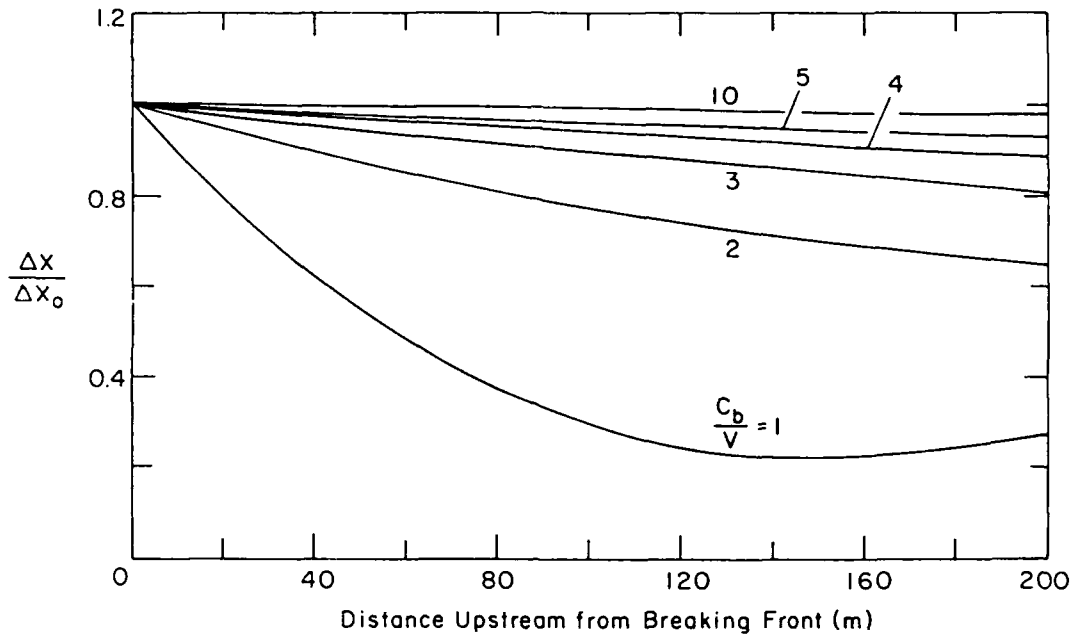

Figure 14. Ice convergence as a function of distance behind the breaking front for a range of dimensionless speeds of the front.

front increases. Paralleling the results at a point, the spatial acceleration relations depicted in Figure 13 indicate that the maximum acceleration occurs at the breaking front for all front speeds, and that the total acceleration decreases more rapidly behind the front as C_b decreases.

Ice convergence is an important characteristic that distinguishes the types of dynamic breakup. When the breaking front passes block i it begins to accelerate. The spacings between this block and its neighbors Δx_{i-1} and Δx_i then begin to change. We will define a quantitative measure of ice convergence as the final block spacing divided by the initial spacing $\Delta x/\Delta x_o$. During breakup this ratio is generally ≤ 1, indicating a reduced ice surface area relative to the initial sheet. This ice convergence measure quantifies the extent of the surface area loss that is necessary for ice continuity.

Ice convergence, like the other parameters of ice motion, also develops a steady state in a coordinate system moving with the breaking front. As before, the results presented in Figure 14 are for a range of dimensionless breaking front speeds. Ice convergence occurs everywhere in the moving pack, and generally increases with distance behind the front. The spatial gradient of ice convergence quantifies the local loss of ice surface area per unit length. The maximum spatial gradient occurs immediately behind the breaking front in all cases. It decreases significantly as the speed of the front increases. Only when $C_b/V \leq 2$ is the gradient near the front much greater than at other points upstream, and these values are more than an order of magnitude larger than those at $C_b/V \geq 4$. At dimensionless breaking front speeds of less than 1, $\Delta x/\Delta x_o$ can be negative with these ice velocity data, indicating that the relative positions of the ice blocks are interchanged. The combination of large travel time and significant ice convergence occurs at low dimensionless breaking front speeds.

On the Connecticut River the ice convergence near the front was small, as evidenced by minimal ridging within the sheet. These observations match the computed results if the local breaking front speed approached the dynamic wave speed. At the other extreme, as the front speed approaches the flow velocity, the ice convergence becomes large at the breaking front as is typical in strength-dominated breakup. The dimensionless speed of the rubble front on the Connecticut River averaged just under 1.5. Transitions between strength- and support-dominated breakup provide an opportunity for plate collisions and size reduction to occur ahead of an existing rubble front. Therefore, the rubble front speed can exceed the flow velocity when the ice velocity does not, and the separation distance between the breaking and rubble fronts is limited.

CONCLUSIONS

In this report we quantify parameters of the ice motion near the breaking front for dynamic breakup of a river ice cover. Dynamic breakup of river ice is generally accompanied by large and rapid changes in both the river flow and the ice motion. The concept of the breaking front as the boundary between moving and stationary ice, and the motion of the ice behind it have been investigated using data from the Connecticut River. Our analysis required the assumptions of constant breaking front speed through a short river reach and identical ice velocity behavior at each point in the reach.

The ice motion was initially studied from the perspective of a stationary observer on the river bank. The ice acceleration was discontinuous with the passage of the breaking front, going from zero to the peak value, and total acceleration was related to local acceleration by the parameter $(1 - v_I/C_b)$. The hydraulic radius associated with the ice diminished dramatically during the initial 60 s of the ice motion, indicating a rapid decrease in the flow resistance of the ice. An equation of motion for the ice and solutions of this equation with constant parameters were developed. Equilibrium ice velocity occurs during steady motion and is a function of bank stress. When the ice motion is unsteady, oscillations in the ice velocity do not occur. The observed ice velocity oscillations require forcing, and the most likely cause of this forcing is variable bank resistance. If all other parameters are the same, the rate of approach to equilibrium increases as the speed of the breaking front decreases.

The ice motion was also observed from the breaking front over a range of dimensionless front speeds to quantify the spatial variations of conditions near the front. Immediately behind the front the time of ice motion, velocity, acceleration and convergence do not vary with time but are strongly related to the speed of the front. As the speed of the breaking front decreases, the time of ice motion at a given distance upstream of the front increases. Ice convergence occurred everywhere in the moving pack, but it was always at a minimum immediately adjacent to the front. As the speed of the front approached the downstream dynamic wave speed C_d, the ice convergence was small over a significant distance upstream of the front. Minimal ice convergence near the front indicates that ice continuity can be satisfied without the development of ridges or other features that are obvious to an observer. If the speed of the breaking front is less than or equal to the ice velocity, the ice convergence near the front is large and the location of the front is distinct.

Minimal ice convergence, short travel times and large block sizes near the breaking front are typical of support-dominated breakup. These characteristics, observed at the ice velocity measurement site, are consistent with this analysis for $C_b \approx C_d >> V_I$. Conversely, this analysis indicates that if $C_b \approx V_I << C_d$, the ice convergence and time of ice motion are large and block sizes are small near the front, characteristics that are typical of strength-dominated breakup.

LITERATURE CITED

Beltaos, S. and B.G. Krishnappan (1982) Surges from ice jam releases: A case study. *Canadian Journal of Civil Engineering*, **9:** 276–284.

Billfalk, L. (1982) Breakup of solid ice covers due to rapid water level variations. U.S. Army Cold Regions Research and Engineering Laboratory, CRREL Report 82-3.

Conte, S.D. and C. deBoor (1980) *Elementary Numerical Analysis: An Algorithmic Approach*, 3rd Edition, New York: McGraw-Hill, p. 251–267.

Doyle, P.F. and D.D. Andres (1979) Spring breakup and ice jamming on the Athabasca River near Fort McMurray. Transportation and Surface Water Engineering Division, Alberta Research Council, Edmonton, Report SWE-79-05.

Ferrick, M.G. and N.D. Mulherin (1989) Framework for control of dynamic ice breakup by river regulation. U.S.A. Cold Regions Research and Engineering Laboratory, CRREL Report 89-12.

Henderson, F.M. and R. Gerard (1981) Flood waves caused by ice jam formation and failure. In *Proceedings of the IAHR Symposium on Ice*, Quebec City, P.Q., Canada, p. 209–219.

Prowse, T.D., J.C. Anderson and R.L. Smith (1986) Discharge measurement during river ice breakup. In *Proceedings of the 43rd Eastern Snow Conference*, Hanover, New Hampshire, p. 55–69.

Wake, A., Y.K. Poon and R. Crissman (1987) Ice transport by wind, wave, and currents. *ASCE Journal of Cold Regions Engineering*, **1**(2): 89–103.

Williamson, D. (1989) Unsteady flow aspects of river ice breakup. MS thesis (unpublished), Dept. of Civil Engineering, University of Alberta, Edmonton.

APPENDIX: ORTHOGONAL POLYNOMIALS

In the following discussion we summarize a more detailed treatment of orthogonal polynomials by Conte and deBoor (1980) and apply it to fitting our ice velocity data. Orthogonal polynomials offer several advantages for fitting data. The property of orthogonality avoids the condition problem in the normal equations that yields poor least-squares approximations. These polynomials satisfy a recurrence relation between the next higher degree polynomial and the two previous polynomials in the sequence, allowing progressive development with great efficiency. The error between the composite polynomial and the data is represented by a time series for each level of the approximation. By comparing the amplitude and structure of the error it is relatively easy to assess the advantage of higher degree approximations. Finally, these polynomials are readily integrated and differentiated.

The ice velocity data were obtained at discrete times in the interval $(0, t_{max})$. A positive weighting function $w(t)$ is defined on this interval, and a scalar product between the arbitrary functions g and h can be defined as

$$< g,h > = \sum_{n=1}^{N} g(t_n)\, h(t_n) w(t_n) \qquad \text{(A1)}$$

where $t_1, t_2, \ldots, t_N$ are fixed times on the interval. The functions $g(t_n)$ and $h(t_n)$ are orthogonal on this interval if $<g,h>=0$. Given that the polynomials $P_0(t), P_1(t), P_2(t), \ldots$ are all orthogonal to each other and that each P_i is a polynomial of exact degree i, then any polynomial $v_I(t)$ of degree $\leq k$ can be written as

$$v_I(t) = d_0 P_0(t) + d_1 P_1(t) + \ldots + d_k P_k(t) \qquad \text{(A2)}$$

with coefficients $d_0, d_1, \ldots, d_k$ uniquely determined by $v_I(t)$.

In our analysis we will obtain a composite polynomial $v_I(t)$ that is equivalent to eq A2 and provides the best least squares approximation of the ice velocity data. We can express the squared error in the polynomial approximation as

$$< f(t) - v_I(t), f(t) - v_I(t) > = \sum_{n=1}^{N} [f(t_n) - v_I(t_n)]^2 w(t_n) \qquad \text{(A3)}$$

and seek a polynomial of degree k that minimizes this error. The ice velocity at $t = 0$ is well known $[f(0) = 0]$ compared to the other data. Therefore, we specify that all the data receive equal weighting and require that $v_I(0)$ be sufficiently close to zero by giving that point a greater weight,

$$w(0) >> 1$$
$$w(t_n) = 1 \qquad , 0 < t_n \leq t_{max}$$

Larger values of $w(0)$ decrease the error at $t = 0$, but the other errors generally increase. Substituting eq A2 into eq A3 yields the error E as a function of the coefficients $d_0, \ldots, d_k$:

$$E(d_0, \ldots, d_k) = < f(t) - d_0 P_0 - \ldots - d_k P_k, f(t) - d_0 P_0 - \ldots - d_k P_k > \qquad \text{(A4)}$$

To minimize E we take $\nabla E = 0$ and obtain

$$\sum_{n=1}^{N} [f(t_n) - v_I(t_n)] w(t_n)\, P_i = 0$$

or equivalently because the polynomials are orthogonal,

$$< P_i, f > = < P_i, v_I > = < P_i, P_i > d_i^* \qquad \text{(A5)}$$

where the * notation indicates the best coefficients. Rearranging eq A5 we obtain

$$d_i^* = \frac{< P_i, f >}{< P_i, P_i >} = \frac{< P_i, f >}{S_i} \qquad \text{(A6)}$$

The set of orthogonal polynomials is developed from the three-term recurrence relation

$$P_{i+1} = (t - B_i) P_i - C_i P_{i-1} \qquad \text{(A7)}$$

with

$$B_i = \frac{< t P_i, P_i >}{S_i} \text{ for } i = 0, 1, 2, \ldots, k-1$$

and

$$C_i = \frac{S_i}{S_{i-1}} \text{ for } i = 1, 2, \ldots, k-1$$

Equations A6 and A7 require that

$$S_i = \sum_{n=1}^{N} [P_i(t_n)]^2 w(t_n) \neq 0 \qquad \text{(A8)}$$

To initiate the polynomial sequence we define

$$P_{-1}(t) = 0$$

$$P_0(t) = 1$$

without the loss of generality.

REPORT DOCUMENTATION PAGE

Form Approved
OMB No. 0704-0188

1. AGENCY USE ONLY (Leave blank)	2. REPORT DATE	3. REPORT TYPE AND DATES COVERED
	October 1991	

4. TITLE AND SUBTITLE

Analysis of River Ice Motion Near a Breaking Front

5. FUNDING NUMBERS

PR: 4A762730AT42
TA: CS
WU: 001

6. AUTHORS

M.G. Ferrick, P.B. Weyrick, and S.T. Hunnewell

7. PERFORMING ORGANIZATION NAME(S) AND ADDRESS(ES)

U.S. Army Cold Regions Research and Engineering Laboratory
72 Lyme Road
Hanover, New Hampshire 03755-1290

8. PERFORMING ORGANIZATION REPORT NUMBER

CRREL Report 91-18

9. SPONSORING/MONITORING AGENCY NAME(S) AND ADDRESS(ES)

U.S. Army Cold Regions Research and Engineering Laboratory
72 Lyme Road
Hanover, New Hampshire 03755-1290

Office of the Chief of Engineers
Washington, D.C. 20314

10. SPONSORING/MONITORING AGENCY REPORT NUMBER

11. SUPPLEMENTARY NOTES

12a. DISTRIBUTION/AVAILABILITY STATEMENT

Approved for public release; distribution is unlimited.

Available from NTIS, Springfield, Virginia 22161

12b. DISTRIBUTION CODE

13. ABSTRACT (*Maximum 200 words*)

A quantitative theory of dynamic river ice breakup is not yet available. One of the essential components of such a theory is a description of the ice motion near the breaking front. In this report we develop an analysis of this motion for a specific case that is consistent with observed data. The analysis is generalized by allowing the speed of the breaking front to vary, and the parameters of the ice motion that are obtained represent different dynamic breakup behaviors that have been described previously. The results of the analysis include 1) the hydraulic radius associated with the ice cover and the total ice acceleration as functions of time, 2) the equilibrium ice velocity as a function of bank resistance, and the ice velocity as a function of time for several initial and bank resistance conditions, 3) the time-varying bank resistance at the measurement location, and 4) the time of ice motion, ice velocity, ice acceleration, and the convergence of the moving ice with distance from the breaking front. The measure of ice convergence quantifies the loss of surface area by the sheet that is required for ice continuity, and distinguishes the types of dynamic breakup.

14. SUBJECT TERMS

Breaking front
Dynamic ice breakup
Ice convergence
Ice motion
Orthogonal polynomials
River ice

15. NUMBER OF PAGES
22

16. PRICE CODE

17. SECURITY CLASSIFICATION OF REPORT	18. SECURITY CLASSIFICATION OF THIS PAGE	19. SECURITY CLASSIFICATION OF ABSTRACT	20. LIMITATION OF ABSTRACT
UNCLASSIFIED	UNCLASSIFIED	UNCLASSIFIED	UL